

# Spatial and Spectral Distributed Multi Population Rate Equations Model for Quantum Dot Superluminescent Diodes

Mariangela Gioannini, Ivo Montrosset

Dipartimento di Elettronica, Politecnico di Torino, mariangela.gioannini@polito.it

**Abstract:** *We present a spectral model of the emission characteristics of quantum dot superluminescent diodes including the influence of residual facet reflectivity. We analyze the transition from the amplified spontaneous emission to lasing regime and the characteristics of multi-section devices with improved performance.*

## Introduction

Superluminescent light emitting diodes (SLD) offer the prospect of high power and wide bandwidth sources for various sensing and spectroscopy applications and in particular for optical coherent tomography, where it is required broad band and very bright light sources with a short temporal coherence. In the last years the Quantum Dot (QD) semiconductor materials have been promising used for the realization of QD-SLD [1,2], thanks to the possibility of tailoring the optical gain bandwidth with a proper engineering of the QD size and composition. Very recently multi-section QD-SLDs [3] have been proposed as a viable solution for the realization of devices with very high power and simultaneously broad band emission. A detailed numerical model for the analysis and the design of bulk SLD has been recently presented in [4], but to our knowledge only simple models have been reported for the case of QD semiconductor material [1].

The model we present in this work takes into account all the peculiar characteristics of the QD material and allows simulating the non-idealities of the device. From the material point of view we include the non-homogeneous distribution of the dot size (inhomogeneous gain broadening) and the presence of other states (wetting layer and SCH states) besides the states confined in the QDs (ground state, GS, and excited state, ES) to calculate the spectral characteristics of the emitted photons. From the device point of view we take into account the longitudinal spatial hole burning effect that is particularly strong in SLD and the effect of non zero reflectivity at the facets. We can therefore predict the amount of ripple in the output spectrum and the condition at which the transition from the SLD to the laser behavior occurs. A proper SLD model has therefore to be able to simulate the effect of the unwanted facet reflectivity and to calculate the output spectrum and the power versus current characteristics including the longitudinal spatial hole burning and the spectral hole burning effects caused by finite carrier capture/escape times in/from

the various QDs of different size.

The paper is organized as follow: we will briefly describe the numerical model used and then we will validate it in a test case, comparing the characteristics of an ideal SLD (zero-facet reflectivity) with those of a laser (as cleaved facet reflectivity). We will then show how the model can be used to analyze some SLD realistic structure. In particular we will analyze the effect of residual facet reflectivity due to non-ideal anti-reflection coating and we will give two examples of analysis of multi-section SLDs.

## Numerical model

The numerical model is based on a traveling power approach: the device is divided in several sections whose photon densities are obtained from the propagation of the forward and backward photons of the two nearest sections. Given the importance of the SLD emission spectra in practical applications, the model is also based on a spectral slicing approach [5]. In each longitudinal section of the device the model calculate the local true spontaneous emission (TSE) and the gain spectra solving a Multi Population Rate Equation system [6]. With this modeling the non-uniform QD ensemble is represented by several sub-groups of QDs, coupled through the wetting layer via the carrier capture and escape process. Each  $n$ -th QD group has different GS and ES energies ( $E_n$ ) and its carrier density is depleted by the stimulated emission of the photons of that section (spatial hole burning). The various QD sub-groups are also coupled together via the homogeneous broadening of the emitted photons (spectral hole burning) that appear in the stimulated emission term. The TSE obtained by the carrier occupation of the various states is then sliced in several energy intervals with sampling step  $\Delta E$ . In equation (1) we report the expression of the TSE emission rate at the central energy  $E_k$  of the  $k$ -th energy interval evaluated in the  $z$  section of the device:

$$R_{sp}(z, E_k) = \sum_{GS, ES} \mu_{GS, ES} N_D n_L C_{spont} \sum_n f_{n, GS, ES}^2(z) \cdot \rho_{opt}(E_n) \cdot G_n \cdot L(E_n - E_k) \quad (1)$$

where  $\mu_{GS, ES}$  is the state degeneracy,  $N_D$  is the QD density per layer,  $n_L$  the number of QD layers,  $C_{spont}$  is a coefficient [6],  $\rho_{opt}(E_n)$  is the density of the optical modes,  $f_{n, ES, GS}^2$  is the occupation probability of the GS/ES of  $n$ -th QD population in the  $z$  section and is obtained solving the MPRE system [6]. In expression (1)  $G_n$  is the existence probability of the  $n$ -th QD population that accounts for the inhomogeneous QD distribution and  $L(E_n - E_k)$  is the homogeneous

broadening function.

The photon density in the forward ( $S_f$ ) and reverse ( $S_r$ ) direction are then given by:

$$S_{f,r}(z, E_k) = S_{f,r}(z, E_k) \cdot \exp(g(z, E_k) \cdot \Delta z) + 0.5 \cdot \beta_{sp} \cdot \frac{\Delta z^2}{v_g} \cdot R_{sp}(z, E_k) \cdot \Delta E_k$$

Where  $g(E_k)$  is the gain spectrum calculated in [6],  $\Delta z$  is the sampling step in the longitudinal direction,  $v_g$  is the group velocity and  $\beta_{sp}$  is the amount of TSE coupled with the guided mode. In the first and last section of the device we add to the term reported above also the contribution of the reverse/forward fields reflected back in the cavity.

Solving the MPRE model in each  $z$  section we therefore account for the spatial hole burning effect in the longitudinal direction of the SLD and we can calculate how much the carrier population in the GS and ES are depleted by the propagating photons in the various sections.

**Numerical results**

The numerical model presented above has been validated analyzing first two test structures with the purpose of showing how the model can simulated a device with any value of end facet reflectivity and therefore account of both amplified spontaneous emission and lasing regimes. At this purpose we have considered a device with as cleaved facet reflectivity (laser, LD, behavior) and a device with zero facet reflectivity (ideal SLD behavior).

**Comparison between laser and SLD behavior**

We consider for the comparison two InAs/GaAs 4.5 mm long QD devices. We compare in the inset of Fig.1a the calculated output power versus current characteristics while in Figs. 1a and 1b are reported the output emission spectra for the two cases at various level of current injection. The spectrum at the highest current in Fig.1, just above LD GS threshold, clearly shows a sharp peak around the GS emission while the SLD spectrum shows a dominant GS emission. The cavity gain in Fig. 2 ( a- for the LD and b- for the SLD) helps in this interpretation because the modal gain around the GS emission is clamped in the LD case whereas, in the SLD case, it presents a maximum. Increasing the current (Figs. 1b and 2a) the LD spectrum broadens and then also the ES start lasing. On the contrary, for the SLD the ES emission becomes first equal to GS emission and then dominates since the GS starts saturating. This behavior has been measured in actual SLD and LD. Fig. 3 reports the calculated normalized longitudinal photon density distribution at the wavelengths corresponding to the GS (dashed line) and ES (solid line) output power spectral peak wavelengths. The strong longitudinal field variation in the SLD case justify the need to use

a longitudinally discretized model to correctly represent the high injection regime, whereas, as it is well known, this is not strictly necessary in a laser except when the ratio of the two reflectivity is high.

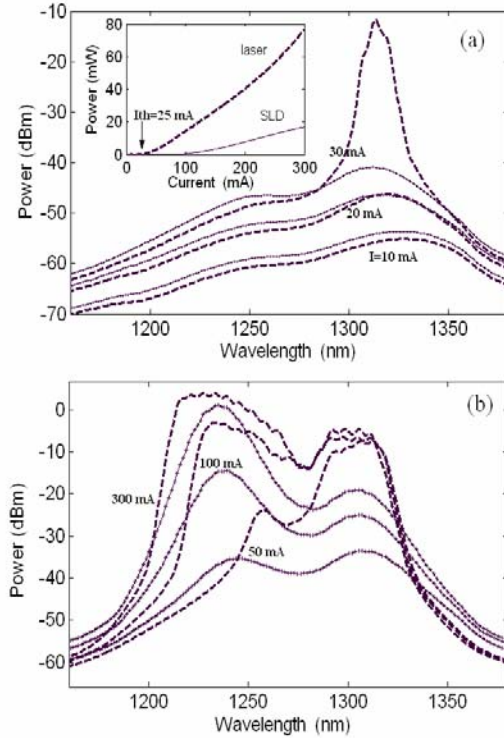


**Fig. 1:** P-I (a) and the spectral (a and b) characteristic of a SLD with zero (continuous lines) and with cleaved (dashed lines) facets reflectivity.

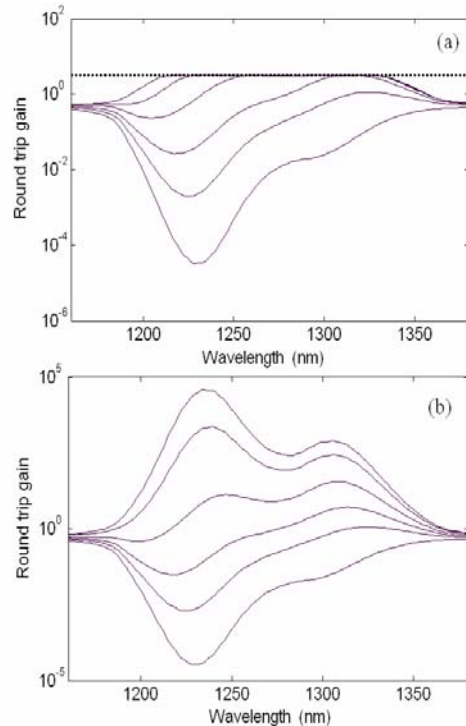


**Fig. 2:** Device round trip gain for the two cases of Fig.1. (a) cleaved FP cavity and (b) ideal SLD. The current levels of each curve are the same of Fig.1.

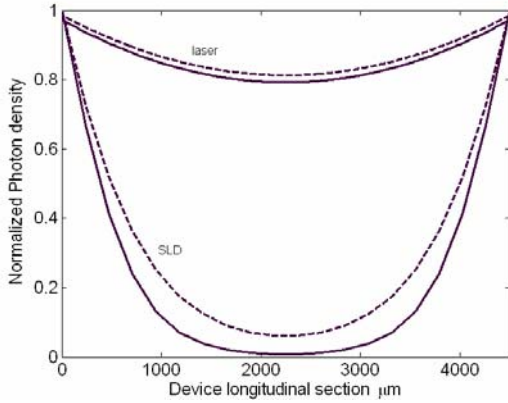


**Fig. 3:** Normalized longitudinal photon distribution at the peak emission wavelengths (GS – dashed and ES- continuous lines) for the ideal SLD and for the FP LD.

**SLD with non-zero facet reflectivity**

In this section we report an example of simulation results of a SLD with non-zero facet reflectivity. We assume that the two facets have a residual reflectivity of  $3 \cdot 10^{-4}$  due to the non-ideal anti-reflection coating. In Fig. 4 we report the calculated power versus current curve and the maximum ripple of the output spectrum evaluated at the peak of the GS and ES emission. The figure shows that the ripple remains low for the GS because the GS gain saturates at quite low values (see Fig. 2b), but it significantly increases for the ES emission. The strong ES ripple at  $I=150$  mA evidence that the ES is getting close to the threshold condition. This result shows that if low ripple values are required (e.g.  $< 3$ dB), the SLD output power is significantly reduced.

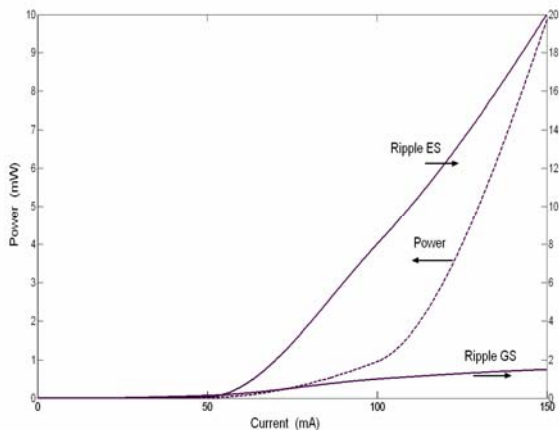


**Fig. 4:** Power versus current characteristic and maximum ripple in the output spectrum at the GS and ES peak emission wavelength. The residual reflectivity of the SLD is set to  $3 \cdot 10^{-4}$

**Analysis of multi-section SLD**

The present model has therefore been used to analyze

from a theoretical point of view various solutions presented in the literature to suppress the residual reflectivity [3,7] and/or increase the output power and emission bandwidth [3]. In all the cases the SLD is divided in two or more sections injected with different current levels.

In this section we analyze two examples of two sections SLD: in the first example we study a SLD with an active plus an absorber section, in the second example we analyze a SLD with two active sections pumped with different current.

The addition of the saturable absorber section was proposed several years ago [7] to suppress the lasing in bulk SLD and applied to the QD case in [3]. The purpose of this example is to show that, in the QD case, when the power in the active section increases, the absorber, being optically pumped by the generated photons, has first a reduction of the absorption and then a transition to a gain condition. In this example we consider a 3 mm long active section followed by 1.5 mm absorber with zero injected current. The facets are as cleaved. We ran several simulations keeping null the current injected in the absorber section and varying the current injected in the active section. We have observed that the many photons emitted by the ES in the active section pump first the carriers in the ES of the absorber; then these carriers relax in the GS giving an increasing of the GS carrier density. The consequence of this behavior is shown in Fig. 5, where we report the average gain of the absorber at the various current injected in the active section. The figure demonstrates that both GS and ES absorption gets smaller and smaller. However, differently from quantum well and bulk saturable absorbers, the GS absorption is not clamped to transparency, but, being refilled from the ES, it can reach a positive gain condition. As a consequence the suppression of the facet reflectivity is reduced more and more and eventually the device starts lasing first from the GS and then also from the ES.

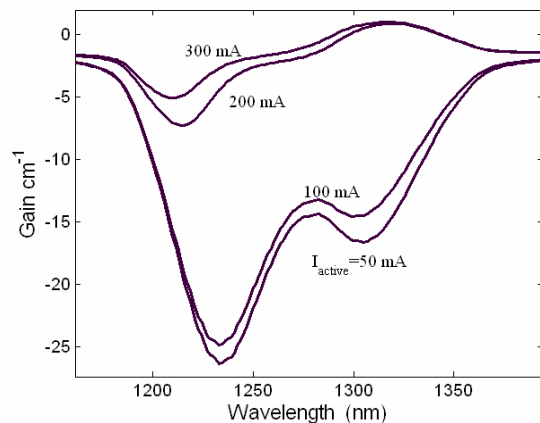


**Fig. 5:** Average gain in the absorber section as function of the current injected in the active section.

In the second example we analyze the output characteristics of a SLD divided in two active sections in-

jected with different currents and with ideally zero facet reflectivity. In this case the first section (1.5 mm with 20 mA current injection) provides the GS power; the second section (3 mm with 450 mA injection) amplifies the GS emission provided by the first section and also generates the ES power. In Fig. 6 we compare the output spectrum of the two section SLD with the one of a 3 mm uniform SLD obtained injecting the same current density. In the two sections case the GS power is suppressed of only 3.7 dB, whereas in the one section design the GS output power is suppressed of more than 9 dB. This example shows that the multi-section SLD design is a viable solution for optimizing the emission bandwidth and output power of these devices.

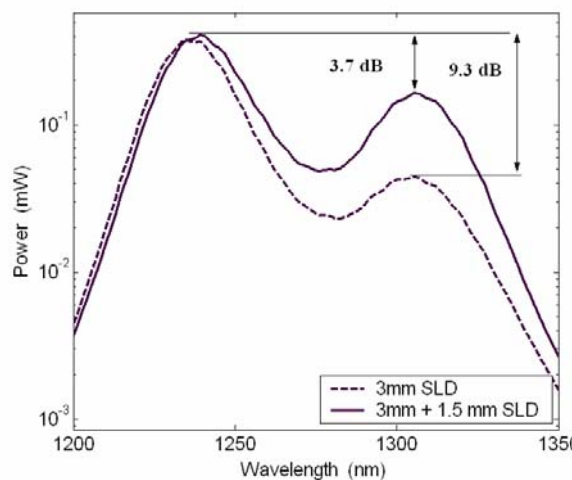


**Fig. 6:** Comparison between the output spectra of one section SLD (dashed line) and two section SLD (solid line).

## Conclusion

We have presented a numerical model for the analysis of QD-SLD. The model includes the inhomogeneous gain broadening due to the QD material, the spectral and spatial hole burning effect and the influence of non null end facet reflectivity. We have demonstrated that the model can account for the transition from the amplified spontaneous emission regime to the lasing regime and it can be used to predict the amount of ripple in the SLD output spectrum. We have also given two examples of analysis of multi-section SLD showing that the present model could be used to test the viability of new design solution of SLD with improved spectral performance.

## Acknowledgments

The author acknowledge the support of the EC IST-NMP-3 STREP project NANO UB-SOURCES.

## References

- 1 M. Rossetti, A. Markus, A. Fiore, L. Occhi, C. Velez, "Quantum dot superluminescent diodes emitting at 1.3  $\mu\text{m}$ ", IEEE Photon. Tech. Lett., no. 3, pp. 540-542, 2005.
- 2 S.K. Ray, K.M.Groom, H.Y. Liu, M. Hopkison, R.A. Hogg, "High power 1.3  $\mu\text{m}$  quantum dot superluminescent diodes", Photonics West, January 2006.
- 3 S.K. Ray, K.M.Groom, H.Y. Liu, M. Hopkison, R.A. Hogg, "High power 1.3  $\mu\text{m}$  quantum dot superluminescent diodes", Photonics West, January 2006.
- 3 Y.C. Xin, A. Martinez, T. Saiz, T.A. Nilsen, A-Moscho, Y. Li, A.L. Gray, A. Vahktin, L.F. Lester, "Novel quantum dot 3-section superluminescent diode", International Conference on Solid State Devices and Materials, Paper B-6-3, Yokohama (Japan), 2006
- 4 J. Park, X. Li, "Theoretical and numerical analysis of superluminescent diodes", IEEE J. Light. Tech., no. 6, pp. 2473-2479, 2006.
- 5 J. Park, X. Li, W.P. Huang, "Comparative study of mixed frequency-time domain models of semiconductor optical amplifiers", IEE Proc. Optoelectron., no. 3, pp. 151-159, 2006.
- 6 M. Gioannini, A. Sevega, I. Montrosset, "Simulation of differential and linewidth enhancement factor of quantum dot semiconductor lasers", Springer Optical and Quantum Electronics, no. 4-6, pp. 381-394, 2006.
- 7 N.S.K. Kwong, K.Y. Lau, N. Bar-Chaim, "High power high efficiency GaAlAs superluminescent diodes with an internal absorber for lasing suppression", IEEE J. Quantum Electron., no. 4, pp. 696-704, 1989.